

MEASUREMENT OF INTENSITIES OF MULTIPLETS IN THE $2\nu_3$ -BAND OF METHANE AT LOW TEMPERATURES*†

SUNIL SARANGI and PRASAD VARANASI

Department of Mechanics, State University of New York at Stony Brook, Stony Brook,
New York 11790, U.S.A.

Abstract—The integrated intensities of the multiplets $P(1)$ – $P(10)$, $R(0)$ – $R(9)$, and of the Q -branch in the $2\nu_3$ -band of $^{12}\text{CH}_4$ have been measured at 102°K, 152°K, 202°K, 251°K, and 300°K. Comparison of our data with theoretical line strengths confirms, at all of the temperatures mentioned, the intensity anomalies observed by MARGOLIS⁽⁵⁾ for lines in this band. The integrated intensity of the $2\nu_3$ -band is found to be $S_\nu = (1.76 \pm 0.04)(300/T \text{ (°K)}) \text{ cm}^{-2} \text{ atm}^{-1}$.

INTRODUCTION

IN A SEQUENCE of three papers,⁽¹⁻³⁾ we reported results of our experimental studies on rotational lines in the ν_3 fundamental^(1,3) and in the ν_4 fundamental⁽²⁾ of methane. In the third paper,⁽³⁾ we also showed how the dependence upon temperature of the intensities and half-widths of $R(0)$, $R(1)$ and $R(2)$ in the ν_3 fundamental can be determined by measuring these parameters at several temperatures between 82°K and 295°K. In the present paper, we report measurements on the $2\nu_3$ -band of methane. In contrast to the work reported in Ref. (3), the present work is not limited to the first three lines in the R -branch, but extends over all the lines between $P(10)$ and $R(9)$ and includes the Q branch as well. The experimental data consist of intensities of all the J -multiplets mentioned, at five temperatures between 100°K and 300°K. The present investigation is intended to serve a dual purpose. Firstly, this band of methane is often the band studied in determining the abundance of this molecule in the atmosphere of the earth.⁽⁴⁾ Secondly, it is worthwhile to compare the various line shape parameters in the ν_3 -fundamental with their counterparts in the overtone of this band, in an attempt to understand any dependence on the vibrational quantum numbers.

During the data reduction stage of our investigation, we noted the recent paper by MARGOLIS.⁽⁵⁾ His measurements at room temperature of the intensities of the J -multiplets in the $2\nu_3$ band agree well with our measurements, except in cases of a few lines which overlap extensively with weak lines belonging to some unidentified methane bands in the region. It is interesting to point out the difference in the techniques employed by Margolis and by us. Margolis studied the multiplets under conditions when the individual components in a multiplet are Doppler-broadened lines or Voigt lines. On the other hand, our measurements have been made on pressure-broadened, and totally blended, multiplets.

* Supported by NASA under grant NGR33-015-139.

† Portions of this work were presented at the 28th Symposium on Molecular Structure and Spectroscopy held at the Ohio State University, Columbus, in June 1973.

Our data, as well as those of Margolis, are in severe disagreement with the earlier intensity measurements of GOLDBERG *et al.*⁽⁶⁾ and of FINK *et al.*⁽⁴⁾ The intensities reported by these authors are much lower than those measured by us and by Margolis.

EXPERIMENTAL PROCEDURE

We have employed essentially the same experimental set up which we have described in detail in our earlier papers. A modification of the design of the low temperature absorption cell deserves mention. For the measurements reported in Ref. (3), we used fused quartz windows for the cell as well as for the vacuum shroud. The mounting of the windows onto the cell body was done by using teflon gaskets.* To insure stability and leak-proof seals at low temperatures the fused-quartz windows and the teflon gaskets were replaced by brazed sapphire window assemblies. Each of these commercially available (Eimac, Division of Varian) window assemblies consists of a sapphire window mounted on a nickel plated Kovar flange. The other end of the flange is brazed onto a high conductivity copper adapter ring, which, in turn, is heli-arc-welded to the end of the nickel plated copper tube (absorption cell).† The fused quartz windows on the vacuum shroud were also replaced by sapphire.

The spectra were scanned with a spectral resolution that ranged between 0.15 cm^{-1} and 0.20 cm^{-1} and a scanning rate of $1.44\text{ cm}^{-1}/\text{min}$. A signal to noise ratio of 100:1 was achieved by employing a quartz iodide lamp, a 400 Hz mechanical chopper, an indium-arsenide photovoltaic detector that is cooled to liquid-nitrogen temperature and a lock-in amplifier with the time constant set at 100 and 300 msec.

For the studies at room temperature, pure methane and glass absorption cells with infrasil windows were used. The cell lengths were 1.01 cm, 2.01 cm and 4.45 cm.

At lower temperatures, the absorption cell described above was used. The length of the low-temperature absorption cell is 10.16 cm. Thus, in order to maintain the lines of $2\nu_3$ band in the linear region of the curve of growth, methane samples were diluted with hydrogen. The percentage of methane in these mixtures was 5.37, 9.81 and 20.29 by volume. The total pressure was varied between 0.5 and 2 atm.

At every temperature, each spectral line was measured about five times and the data reported here are averages of all such measurements.

RESULTS AND DISCUSSION

The intensity data presented in Table 1 and in Figs. 1, 2, and 3 were derived by employing a curve of growth procedure. With the exception of the singlets $R(0)$ and $R(1)$ and the practically coincident doublet $R(2)$, all of the other vibration-rotation transitions in the $2\nu_3$ band of methane are multiplets. The only other singlet in the band is $P(1)$ which, except at temperatures of 100°K and lower, is very difficult to distinguish from the Q branch. The curve-of-growth procedure employed by us for the multiplets was somewhat less direct than that used for singlets. For singlets, we merely used the Ladenburg-Reiche curve. For multiplets, this curve is obviously not applicable. It would have been desirable to measure absorption by each multiplet in the linear region of the curve-of-growth so that the intensity of the multiplet can be measured without resorting to assumptions on the shapes and relative intensities of the individual components of each multiplet. However, in practice, we have

* In Ref. (3) we stated erroneously that indium gaskets were used to seal the cell.

† We thank Mr. William Wilkes of Eimac, Division of Varian for making these window assemblies for us.

Line	$T = 102^\circ\text{K}$	152°K	202°K	251°K	300°K
$P(10)$		0.0335 (13)	0.0362 (12)	0.0389 (19)	
$P(9)$		0.0260 (15)	0.0334 (19)	0.0388 (12)	0.0382 (07)
$P(8)$		0.0357 (11)	0.0418 (13)	0.0408 (11)	0.0399 (01)
$P(7)$	0.0419 (29)	0.0594 (23)	0.0599 (15)	0.0534 (11)	0.0455 (03)
$P(6)$	0.1112 (37)	0.1147 (25)	0.0911 (20)	0.0778 (13)	0.0609 (11)
$P(5)$	0.1216 (33)	0.0951 (52)	0.0640 (45)	0.0494 (24)	0.0386 (15)
$P(4)$	0.2471 (85)	0.1525 (27)	0.0972 (39)	0.0679 (20)	0.0464 (10)
$P(3)$	0.2639 (47)	0.1356 (22)	0.0817 (09)	0.0528 (04)	0.0355 (13)
$P(2)$	0.1205 (24)	0.0536 (11)			
$P(1)$	0.0352 (21)				
$R(0)$	0.2094 (70)	0.0819 (20)	0.0392 (05)	0.0228 (05)	0.0160 (10)
$R(1)$	0.1795 (13)	0.0711 (21)	0.0376 (08)	0.0219 (08)	0.0162 (06)
$R(2)$	0.3151 (130)	0.1440 (60)	0.0795 (09)	0.0507 (11)	0.0354 (07)
$R(3)$	0.5912 (66)	0.2992 (83)	0.1687 (33)	0.1122 (23)	0.0733 (07)
$R(4)$	0.5190 (154)	0.3266 (50)	0.2010 (44)	0.1394 (26)	0.0960 (38)
$R(5)$	0.2726 (67)	0.2066 (50)	0.1490 (44)	0.1124 (27)	0.0807 (24)
$R(6)$	0.2372 (57)	0.2483 (107)	0.1998 (39)	0.1613 (22)	0.1229 (28)
$R(7)$	0.1049 (47)	0.1364 (36)	0.1264 (33)	0.1186 (34)	0.0939 (14)
$R(8)$	0.0754 (38)	0.0883 (74)	0.0985 (57)	0.0940 (32)	0.0839 (27)
$R(9)$	0.0393 (03)	0.0610 (14)	0.0755 (23)	0.0805 (22)	0.0746 (23)
S_{band}	5.151 (126)	3.509 (95)	2.619 (66)	2.147 (49)	1.765 (40)

* Figures in parentheses represent estimated experimental uncertainties (standard deviations) and refer to the corresponding last digits of measured intensities.

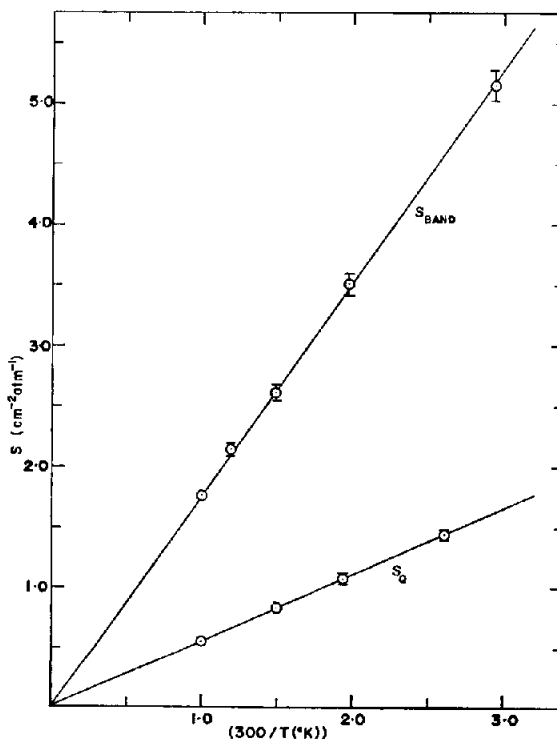


Fig. 1. Integrated band intensity (S_{band}), and intensity of the Q branch (S_Q), as functions of (T^{-1}) yield straight lines, showing that the band intensity per molecule is constant with temperature.

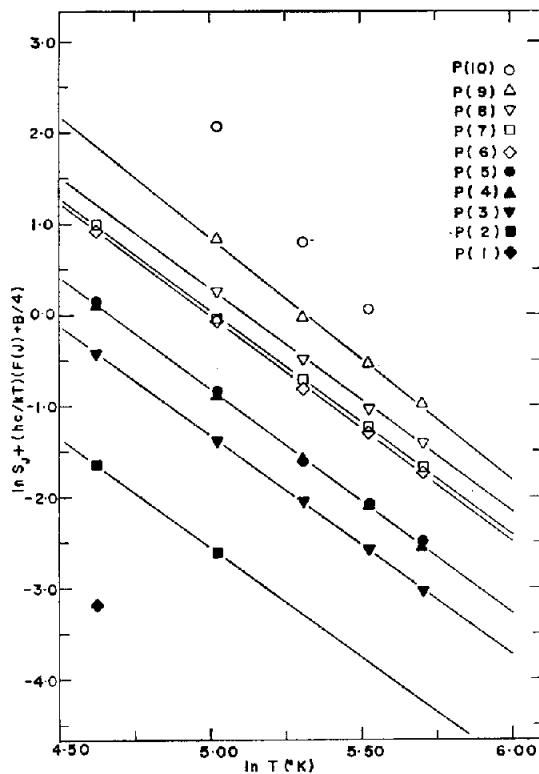


Fig. 2. The points show the relation between line intensity (S_J) and temperature (T) for lines in the P-branch of $2\nu_3$ -band. The straight lines are obtained by a least-square fit to the points.

found the severe accuracy-limitations imposed by the measuring apparatus in the unambiguous determination of equivalent widths make it necessary to study absorption by the lines that is not strictly in the linear region of the curve of growth. Thus, we had to resort to an iterative scheme that would improve upon the preliminary estimates of S_J obtained by using the relation applicable to the linear region: $S_J = (pl)^{-1} W_J$. Here, p (atm) and l (cm) are, respectively, the partial pressure of methane and the cell length that would give rise to an equivalent width W_J (cm^{-1}) for a multiplet of integrated intensity S_J ($\text{cm}^{-2} \text{atm}^{-1}$). Further iteration upon this approximate estimate required a systematic computation of equivalent widths of the multiplets by using the theoretical assignment of lines by BOBIN,⁽⁷⁾ in a manner similar to that described by MARGOLIS.⁽⁵⁾ The essential difference between our computational scheme and that of Margolis is in the shape of the contributing lines. The pressures at which our measurements have been carried out requires using the Lorentz lineshape, while the study by Margolis was on lines with Voigt profiles. In addition to assuming the profiles of the individual components within each multiplet to be Lorentzian, we have also assumed for all of the lines in the present study the following collision-broadened half-widths:⁽³⁾ $\gamma_{\text{CH}_4-\text{CH}_4}^0 = 0.085 (T/295)^{-2/3}$ and $\gamma_{\text{CH}_4-\text{H}_2}^0 = 0.075 (T/295)^{-1/2}$. The iteration scheme and the final value of the multiplet strength S_J are quite insensitive to errors of up to 20 per cent in the half-widths. An IBM 370(155) computer was employed to carry out the iteration which was performed in double-precision and the convergence was

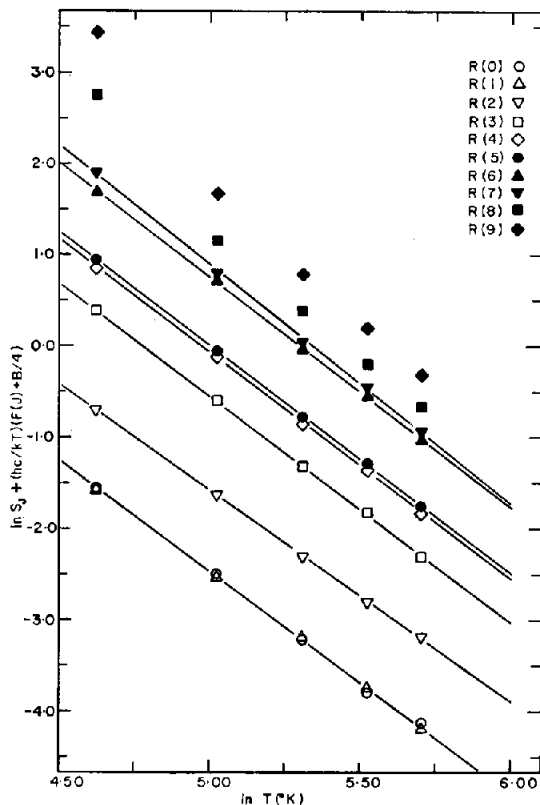


Fig. 3. The points show the relation between line intensity (S_j) and temperature (T) for lines in the R -branch of $2\nu_3$ -band. The straight lines are obtained by a least-square fit to the points.

rapid. The intensities presented in Table 1 represent the averages, at each temperature, of five independent measurements on each multiplet. The quoted limits of error reflect only the standard deviation. We compare in Table 2 our data at room temperature with those of MARGOLIS,⁽⁵⁾ GOLDBERG *et al.*⁽⁶⁾ and FINK *et al.*⁽⁴⁾ Goldberg *et al.* give f -numbers from which we deduced the corresponding line intensities. It is clear from this comparison that the intensities reported by Goldberg *et al.* are significantly lower than those reported by us and by Margolis. Lower estimates for line intensities are often obtained if the measured lines do not fall in the linear part of the curve of growth. Corrections to measured equivalent width can be made only if the line half widths are known *a priori*. It should be remembered that this information was not available at the time the work of Goldberg *et al.* was published. Thus the procedure adopted by Goldberg *et al.* suggests as probable source of error that mentioned above.

From our data on multiplet intensities at 102°K, 152°K, 202°K, 251°K, and 300°K given in Table 1, we have been able to derive the temperature dependence of these intensities and the results are shown in Table 3 and in Figs. 1-3. The integrated intensity data for the Q branch are best represented by the relation

$$S_Q = 0.554 (300/T (^\circ\text{K})) \text{ cm}^{-2} \text{ atm}^{-1}.$$

Table 2. Comparison of the intensities measured at room temperature with previous studies

Line	This study (300°K)	Ref. (5) (300°K)	Ref. (6) (293°K)	Ref. (4) (298°K)
<i>P</i> (9)	0.0382 (07)	0.0328 (27)	0.0229	
<i>P</i> (8)	0.0399 (01)	0.0383 (06)	0.0276	
<i>P</i> (7)	0.0455 (03)	0.0463 (25)	0.0316	
<i>P</i> (6)	0.0609 (11)	0.0570 (40)	0.0452	
<i>P</i> (5)	0.0386 (15)	0.0347 (13)	0.0248	
<i>P</i> (4)	0.0464 (10)	0.0445 (11)	0.0355	
<i>P</i> (3)	0.0355 (13)	0.0322 (21)	0.0249	
<i>P</i> (2)		0.0105 (09)	0.0075	0.0085
<i>R</i> (0)	0.0160 (10)	0.0129 (05)	0.0100	0.0095
<i>R</i> (1)	0.0142 (06)	0.0125 (02)	0.0094	
<i>R</i> (2)	0.0354 (07)	0.0294 (16)	0.0216	
<i>R</i> (3)	0.0733 (07)	0.0845 (67)	0.0543	
<i>R</i> (4)	0.0960 (38)	0.0943 (24)	0.0660	
<i>R</i> (5)	0.0807 (24)	0.0717 (10)	0.0608	
<i>R</i> (6)	0.1229 (28)	0.1228 (61)	0.0922	
<i>R</i> (7)	0.0939 (14)	0.0926 (25)	0.0707	
<i>R</i> (8)	0.0839 (27)	0.0784 (12)	0.0617	
<i>R</i> (9)	0.0746 (23)	0.0691 (41)	0.0549	

This simple relation is shown in Fig. 1 along with a plot of the absolute intensity of the entire band S_{band} . The latter was obtained by summing the intensities of all of the measured multiplets (see Table 1) and adding a small contribution that arises from lines with higher rotational quantum numbers by using theoretical estimates. A least-square fit to the band intensity data yields

$$S_{\text{band}} = (1.76 \pm 0.04)(300/T(^{\circ}\text{K})) \text{ cm}^{-2} \text{ atm}^{-1}.$$

The relation between the integrated intensity of a multiplet and temperature ($^{\circ}\text{K}$) may be written in the form

$$\ln S_j + (hc/kT)[F(J) + B/4] = \alpha \ln T + \beta. \quad (1)$$

Here S_j refers to the total of the integrated intensities of all of the components of a J -multiplet, $F(J)$ the rotational term value of the corresponding lower level and B the rotational constant. α and β are assumed to be constant which can be obtained by fitting equation (1) to the data of Table 1. For a spherical rotor molecule, especially when the band intensity follows a simple T^{-1} dependence upon temperature, one expects α to be equal to $-5/2$.⁽³⁾ One may compare this value with the results, shown in Table 3 and Figs. 2 and 3, of a least-square-fit of equation (1) to the intensity data of Table 1. Only for the multiplets $R(8)$, $R(9)$, and $P(9)$ do we find any significant deviation in α from the value of -2.5 . This may be due to the presence of many weak lines in those spectral regions. This fact is clearly illustrated in Fig. 4. In this figure, we compare the $2\nu_3$ band surveyed at 300°K with the same at 115°K. It appears that, while the lines appearing in the troughs between low J multiplets either disappear or become considerably weaker at the lower temperature, those present in the troughs between $R(8)$ and $R(9)$, and near $P(9)$, become more intense at low temperatures.

It should be mentioned that the estimates we have arrived at for the intensity of $R(2)$ at 202°K, 251°K, and 300°K bear larger uncertainties than at lower temperatures. This is

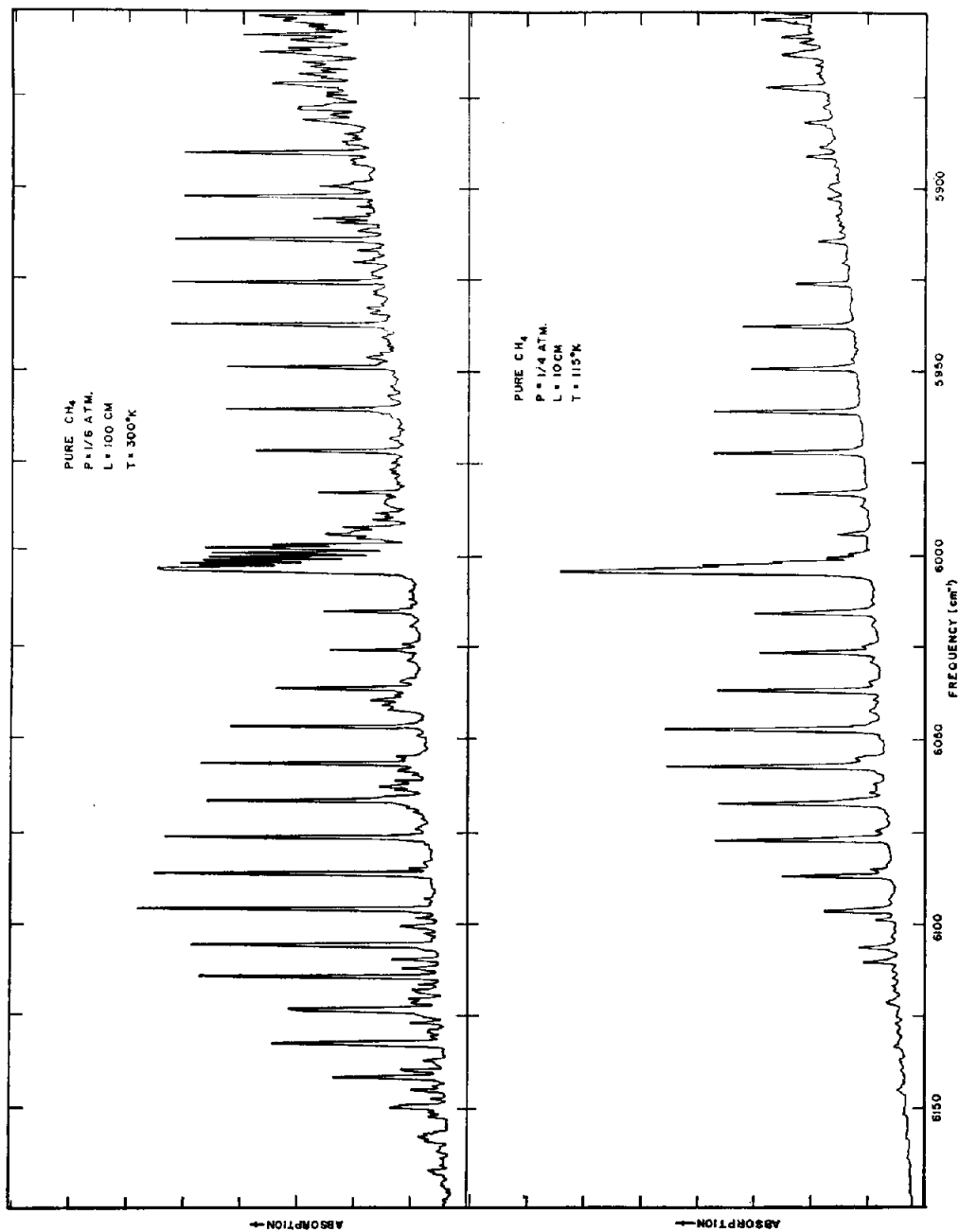


Fig. 4. Survey scans of the $2\nu_3$ -band at 300°K and 115°K show that weak foreign lines are suppressed at reduced temperature.

Table 3. Least-squares-fit of equation (1) to intensity data of Table 1

Line	α	β
<i>P</i> (9)	-2.66	14.14
<i>P</i> (8)	-2.45	12.55
<i>P</i> (7)	-2.46	12.34
<i>P</i> (6)	-2.47	12.32
<i>P</i> (5)	-2.45	11.46
<i>P</i> (4)	-2.45	11.44
<i>P</i> (3)	-2.40	10.67
<i>P</i> (2)	-2.41	9.50
<i>R</i> (0)	-2.43	9.70
<i>R</i> (1)	-2.45	9.77
<i>R</i> (2)	2.32	10.01
<i>R</i> (3)	-2.48	11.84
<i>R</i> (4)	2.48	12.31
<i>R</i> (5)	-2.48	12.39
<i>R</i> (6)	2.51	13.32
<i>R</i> (7)	-2.62	14.00
<i>R</i> (8)	-3.13	17.06
<i>R</i> (9)	-3.44	19.18

apparent in Figs. 8, 9 and 10. Furthermore, in Fig. 4, one can clearly notice the presence of what looks like a *Q* branch of a weak vibrational transition in the vicinity of *R*(2). This fact is further amplified in Fig. 5, where we present two scans of the spectral region around *R*(2) at 300°K and 118°K. It is clearly demonstrated that the *Q* branch present at 300°K disappears at 118°K, thereby lending support to the thought that it perhaps belongs to a weak hot band.

MARGOLIS⁽⁵⁾ has observed at room temperature that measured intensities in the $2\nu_3$ -band deviate from theoretical intensity formulae. He has described this deviation in terms of an empirical Herman-Wallis factor. We have also observed, at every temperature, such systematic deviation from theoretical intensities. We present in Figs. 6-10 the ratios $S(\text{experimental})/S(\text{theoretical})$ obtained at 102°K, 152°K, 202°K, 251°K and 300°K, respectively, for most of the multiplets in the *P* and *R* branches and for the *Q*-branch. There appears to be significant 'borrowing of intensity' by the *R*-branch from the *P* branch as well as from the *Q*-branch. The theoretical analysis of Fox⁽⁸⁾ considers vibration-rotation interaction through a contact transformation of the dipole moment function to second order. We believe that inclusion of higher order terms in the expansion of dipole moment in normal coordinates may partially explain the observed intensity distribution. At this time, however, we can only present an empirical formulation, in which we introduce a factor $\chi(m)$ through the relation

$$\chi(m) = S_m(\text{expt})/S_m(\text{theo}).$$

where $m = J + 1$ for the *R*-branch and $m = -J$ for the *P*-branch. We can subject the data in Figs. 6-10 to least-square fits of the form

$$\chi(m) = a_0 + a_1 m + a_2 m^2, \quad (2)$$

with the *Q* branch identified by $m = 0$. The values of the constants at each temperature are presented in Table 4. It is interesting to note that our value for the constant a_1 agrees well

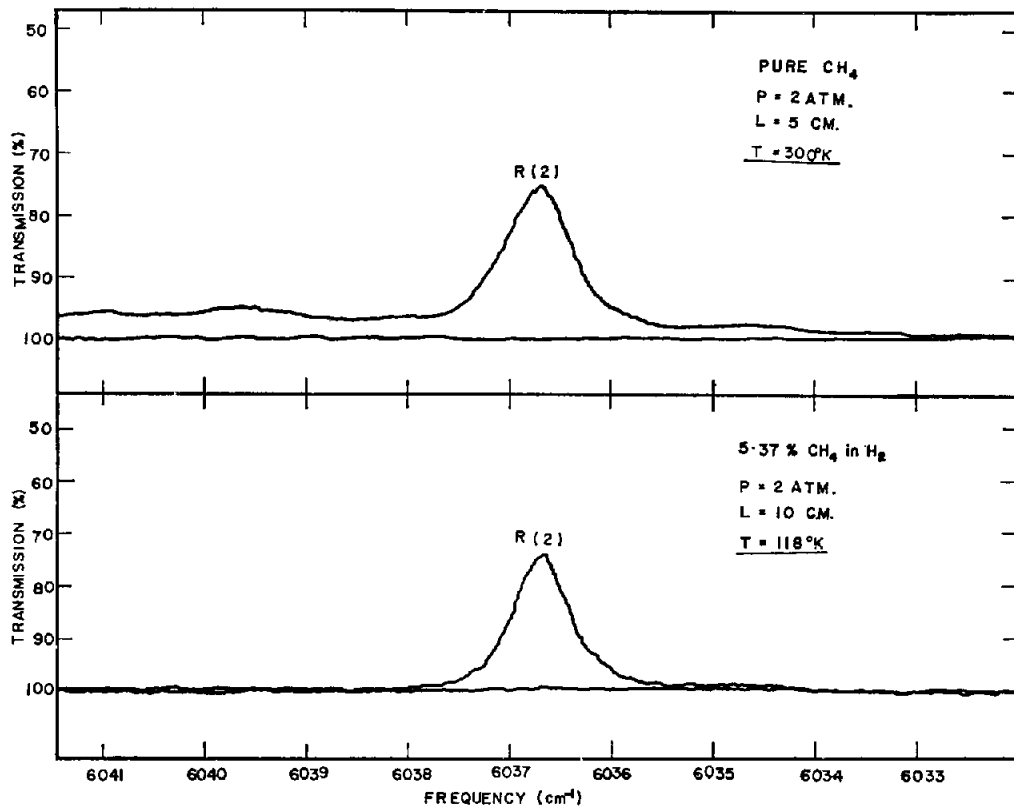


Fig. 5. Scans of the line $R(2)$ of $2\nu_3$ -band at 300°K and 118°K show the presence of weak foreign lines in the wings at room temperature.

Table 4. Least-squares-fit of equation (2) to data from Figs. 6-10

Temperature ($^\circ\text{K}$)	Lines	a_0	a_1	a_2
102	$P(1)-P(7)$	0.920	0.033	0.0017
	Q-branch			
	$R(0)-R(7)$			
152	$P(2)-P(9)$	0.891	0.033	0.0031
	Q-branch			
	$R(0)-R(9)$			
202	$P(3)-P(9)$	0.929	0.031	0.0013
	Q-branch			
	$R(0)-R(9)$			
251	$P(3)-P(9)$	0.947	0.030	0.0009
	Q-branch			
	$R(0)-R(9)$			
300	$P(3)-P(9)$	0.982	0.027	0.0003
	Q-branch			
	$R(0)-R(9)$			

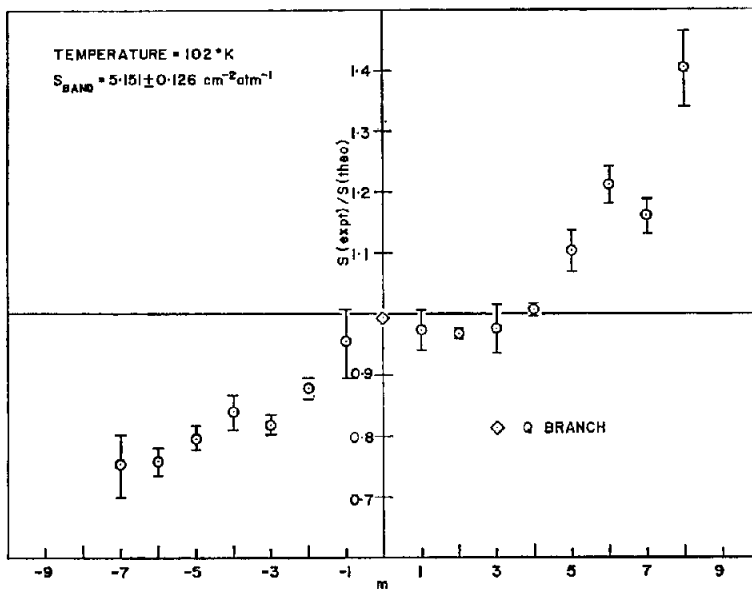


Fig. 6. Plot of $S(\text{exp})/S(\text{theo})$ vs m at 102°K.

with the constant a of Ref. (5), in which a procedure similar to ours has been employed. The constant a_2 , which is quite sensitive to the scatter in the data, differs substantially from the constant b of Ref. (5).

It would certainly be worthwhile to see whether one observes the same anomalies reported

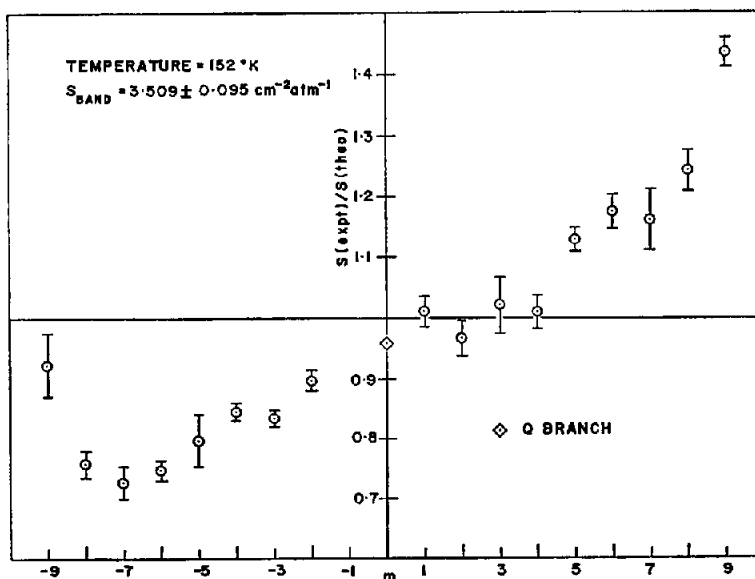


Fig. 7. Plot of $S(\text{exp})/S(\text{theo})$ vs m at 152°K.

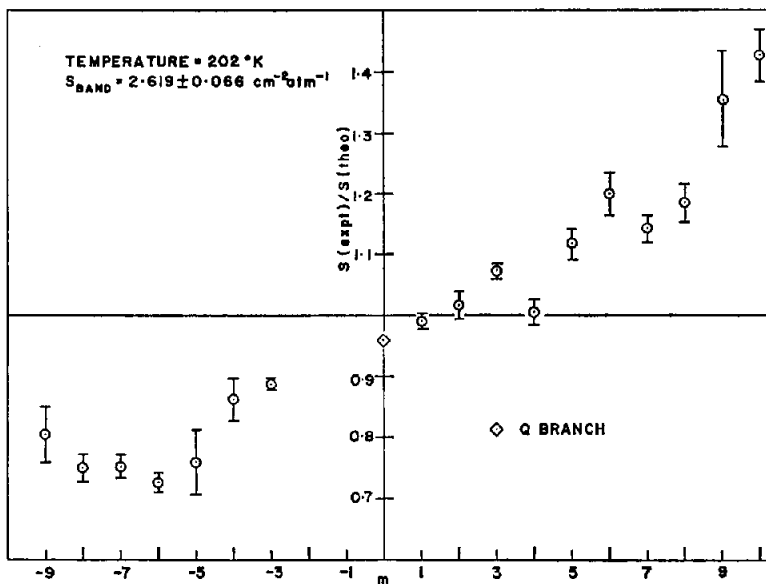


Fig. 8. Plot of $S(\text{expt})/S(\text{theo})$ vs m at 202°K.

here also in the ν_3 -fundamental and other bands of methane. A systematic study of “related” vibrational transitions should provide a key to the nature of this type of vibration-rotation interaction. Such an effort is already in progress and will be reported at a later date.

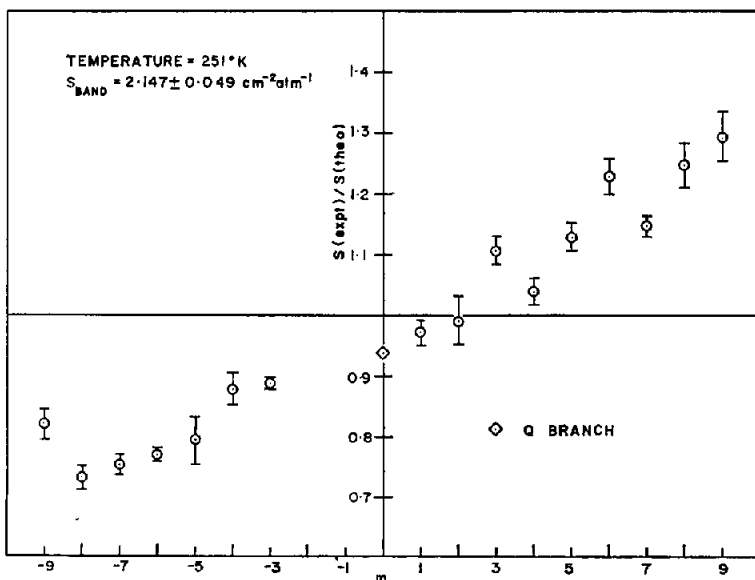


Fig. 9. Plot of $S(\text{expt})/S(\text{theo})$ vs m at 251°K.

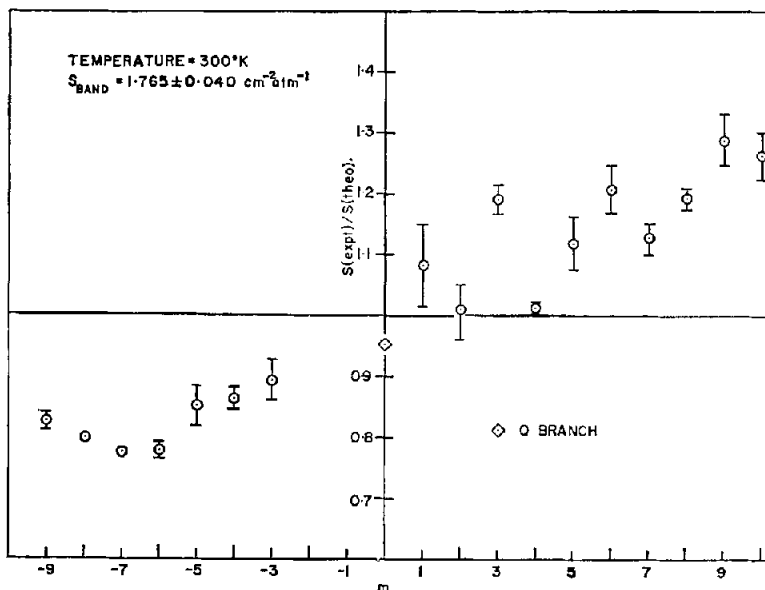


Fig. 10. Plot of $S(\text{expt})/S(\text{theo})$ vs m at 300°K.

Acknowledgement—We are grateful to Dr. JACK MARGOLIS for providing us with a preprint of his paper.

REFERENCES

1. P. VARANASI, *JQSRT* **11**, 1711 (1971).
2. P. VARANASI and G. D. T. TEJWANI *JQRST* **12**, 849 (1972).
3. P. VARANASI, S. SARANGI and L. PUGH, *Astrophys. J.* **179**, 977 (1973).
4. U. FINK, D. H. RANK and T. A. WIGGINS, *J. Opt. Soc. Am.* **54**, 472 (1964).
5. J. S. MARGOLIS, *JQSRT* **13**, 1097 (1973).
6. L. GOLDBERG, O. C. MOHLER and R. E. DONOVAN, *J. Opt. Soc. Am.* **42**, 1 (1951).
7. B. BOBIN, *J. Phys.* **33**, 345 (1972).
8. K. FOX, *J. molec. Spectrosc.* **9**, 381 (1962).